JOURNAL OF VIROLOGY, Apr. 2006, p. 3935–3946 Vol. 80, No. 8
0022-538X/06/$08.00+0 doi:10.1128/JVI.80.8.3935–3946.2006


# Dissecting Rotavirus Particle-Raft Interaction with Small Interfering RNAs: Insights into Rotavirus Transit through the Secretory Pathway

Mariela A. Cuadras,[1,2] Bruno B. Bordier,[1]† Jose L. Zambrano,[4] Juan E. Ludert,[4] and Harry B. Greenberg[1,2,3]*

*Division of Gastroenterology and Hepatology, Department of Medicine,[1] and Department of Microbiology and Immunology,[2] Stanford University School of Medicine, Stanford, California 94305; VA Palo Alto Health Care System, Palo Alto, California 94304[3]; and Laboratorio de Biología de Virus, Centro de Microbiología y Biología Celular, Instituto Venezolano de Investigaciones Científicas (IVIC), Caracas 1020-A, Venezuela[4]*

Received 18 November 2005/Accepted 3 February 2006

**Studies of rotavirus morphogenesis, transport, and release have shown that although these viruses are released from the apical surface of polarized intestinal cells before cellular lysis, they do not follow the classic exocytic pathway. Furthermore, increasing evidence suggests that lipid rafts actively participate in the exit of rotavirus from the infected cell. In this study, we silenced the expression of VP4, VP7, and NSP4 by using small interfering RNAs (siRNAs) and evaluated the effect of shutting down the expression of these proteins on rotavirus-raft interactions. Silencing of VP4 and NSP4 reduced the association of rotavirus particles with rafts; in contrast, inhibition of VP7 synthesis slightly affected the migration of virions into rafts. We found that inhibition of rotavirus migration into lipid rafts, by either siRNAs or tunicamycin, also specifically blocked the targeting of VP4 to rafts, suggesting that the association of VP4 with rafts is mostly mediated by the formation of viral particles in the endoplasmic reticulum (ER). We showed that two populations of VP4 exist, one small population that is independently targeted to rafts and a second large pool of VP4 whose association with rafts is mediated by particle formation in the ER. We also present evidence to support the hypothesis that assembly of VP4 into mature virions takes place in the late stages of transit through the ER. Finally, we analyzed the progression of rotavirus proteins in the exocytic pathway and found that VP4 and virion-assembled VP7 colocalized with ERGIC-53, suggesting that rotavirus particles transit through the intermediate compartment between the ER and the Golgi complex.**

Rotaviruses are the single most important cause of severe diarrhea in infants and young children around the world (35). These viruses are nonenveloped viruses composed of three concentric layers of protein and 11 segments of double-stranded RNA (dsRNA) (14). In vivo, these viruses replicate primarily in the intestinal villus tip epithelial cells of the small bowel, and in vitro, the viral replication cycle has been primarily studied by using a variety of epithelial cell lines of renal or intestinal origin (15).The mechanism underlying rotavirus assembly and release is not totally understood. During maturation, rotavirus double-layer particles (DLPs) bud into the endoplasmic reticulum (ER) by using the virally encoded nonstructural protein NSP4 and acquire an ER-derived lipid membrane that is eventually lost and replaced by two outer capsid proteins, VP7 and VP4 (14). Studies of the transport and release of the rhesus rotavirus (RRV) showed that, before cellular lysis, it leaves polarized intestinal Caco-2 cells almost exclusively from the apical surface by a nonconventional transport pathway that bypasses the Golgi complex (21). In addition, ultrastructural studies revealed smooth vesicles containing mature virions underlining the apical plasma membrane of infected cells, suggesting that vesicular carriers transport virions to the apical surface in rotavirus-infected cells (21). Together, these basic observations led to efforts to characterize the molecular pathways and the cellular machinery involved in rotavirus exit from the infected cell.

Lipid rafts are dynamic microdomains in cellular membranes enriched in sphingolipids and cholesterol that play a critical role in apical membrane trafficking (44). Recently, we demonstrated that rotavirus proteins closely associate with lipid rafts in RRV-infected Caco-2 cells by isolation of these microdomains with cold Triton X-100 (TX-100) and equilibrium centrifugation (9). Additionally, another group showed that mature viral particles and recombinant VP4 interact with model lipid mixtures that resemble rafts and that VP4 from infected cells associates with rafts as early as 6 h postinfection (hpi) (40). Further characterizing the association of RRV with these microdomains during replication, we demonstrated that infectious triple-layer particles (TLPs) accumulate in rafts and that this association takes place intracellularly, both in cell culture and in infected animals (9). Later, Delmas and coworkers, who aimed at determining the site of final assembly of rotavirus, showed that inhibition of glycosylation in Caco-2 cells with tunicamycin (TM) did not interfere with the association of VP4 with rafts, suggesting that VP4 assembly into the viral particle occurs as an extra-ER event (11).

In order to release proteins or molecules into the external medium or to target proteins to the plasma membrane, cells have developed specialized secretory pathways. The early steps of conventional secretion take place in the ER and involve transport of the cargo proteins from the ER through the ER-

* Corresponding author. Mailing address: VAPACHS, 3801 Miranda Ave., MC 154C, Palo Alto, CA 94304. Phone: (650) 493-5000, ext. 63121. Fax: (650) 852-3259. E-mail: hbgreen@stanford.edu.

† Present address: Biolumine SA, UMR CNRS 6144 GEPEA/ERTint 1052 CBAC, Campus de la Courtaisière, Institut Universitaire de Technologie, 85035 La Roche sur Yon, France.

Golgi intermediate compartment (ERGIC) to the Golgi apparatus via a vesicle-mediated transport system (19). The ERGIC is enriched in and can be visualized by a lectin-like transport protein named ERGIC-53 and the COPI coat subunit β-COP, both of which constantly recycle among the ER, the ERGIC, and the Golgi (19). Numerous studies have used colocalization of ERGIC-53 and vesicle markers to help follow trafficking of specific cargo proteins after they leave the ER (1, 18).

Silencing of gene expression by RNA interference (RNAi) has become a powerful experimental tool used to study gene function. This mechanism is activated by dsRNA and involves the generation of small interfering RNAs (siRNAs). Basically, siRNAs homologous to a region of an mRNA are able to initiate specific degradation of the target mRNA, leading to the silencing of its expression (13, 28). Since there is no reverse genetic system available to engineer the genome of infectious rotavirus, RNAi has recently been exploited effectively to characterize the function of several rotavirus genes (10, 26, 27, 43). The formation of particles lacking VP4 with siRNAs suggests that VP4 is essential neither for assembly nor for release of DLPs from the ER (10). In this study, we shut down individual viral mRNAs encoding VP4, VP7, and the multifunctional nonstructural protein NSP4 with siRNAs and evaluated the effect of silencing these viral mRNAs on rotavirus particle-raft interactions in order to better define the role of viral proteins in the targeting of rotavirus to cellular rafts. We found that VP4 siRNA and $NSP4^{219}$ siRNA, but not a VP7 siRNA, substantially reduced the association of rotavirus particles with rafts. Interestingly, our data showed that the inhibition of rotavirus particle migration into lipid rafts by both $NSP4^{219}$ siRNA and TM also acts on the targeting of VP4 to these lipid raft microdomains, supporting the conclusion that the primary association of VP4 with rafts occurs during the initial stage of particle formation in the ER. Additional characterization of the transit of rotavirus through the secretory pathway demonstrated that rotavirus infection induces a reorganization of the ERGIC and that mature rotavirus particles transit through this organelle during their maturation process.

## MATERIALS AND METHODS

**Cell culture and virus replication.** MA104 cells (American Type Culture Collection) were cultured in medium 199 (M199; Invitrogen) supplemented with 10% fetal bovine serum (FBS) at 37°C in 5% $CO_2$. The monoreassortant strain DXRRV, containing gene 9 from the D strain of G1 human rotavirus on a genomic background of RRV (30), was propagated in MA104 cells as previously described (8).

**Metabolic labeling and raft purification from infected cells.** Monolayers of MA104 cells were infected with DXRRV at a multiplicity of infection (MOI) of 10; 7 h after infection, the cells were starved in methionine-free medium for 1 h and labeled for 30 min with 200 μCi/ml of Pro-mix L[$^{35}$S] (Amersham Pharmacia). The labeling medium was washed out, and the cells were incubated for 1 h in chasing medium (M199 supplemented with 1 mM cycloheximide [Calbiochem] and 10 mM L-methionine [Sigma]). At the end of the chase period, the cells were washed three times with ice-cold phosphate-buffered saline (PBS [Invitrogen]), scraped, and recovered by centrifugation. Since rafts are insoluble in nonionic detergents, they were isolated by extraction with cold 1% TX-100 and separated by equilibrium centrifugation in OptiPrep (Sigma) gradients as previously described (9). In some experiments, cells were incubated in medium with 10 mM methyl-β-cyclodextrin (mβcdx) (Sigma) or 10 μg/ml of TM (Calbiochem) 1 h before the labeling period and the drugs were maintained during the course of the experiment.

**Separation of free VP4 from virion-associated VP4 in the raft fraction.** Rafts were isolated from three 175-cm$^2$ flasks of DXRRV-infected MA104 cells as described above; the purified-raft-enriched fraction, fraction 4 (f4) was then diluted and rotavirus particles were pelleted by ultracentrifugation (2 h, 4°C, 178,000 × *g*). The post-ultracentrifugation supernatant (PUSN) was concentrated in a Centriplus YM-10 centrifugal filter device (Amicon; Millipore) according to the manufacturer's recommendations in order that proteins with molecular masses of ≥10,000 Da in the PUSN were recovered. Pelleted material and concentrated PUSN were brought to a final volume of 200 μl, and the presence of VP4 in both samples was detected by sodium dodecyl sulfate-polyacrylamide gel electrophoresis (SDS-PAGE) and immunoblotting. As indicated, half of the volume of the starting raft fraction was solubilized with 60 mM octylglucoside because it is known that this condition solubilizes proteins associated with rafts (4). As a control, semipurified virus (7) was subjected to the same treatment and analyzed by Western blotting.

**SDS-PAGE and Western blotting.** To analyze the $^{35}$S-labeled proteins, an aliquot of each gradient fraction was subjected to gel electrophoresis in 10% Bis-Tris gels (NuPAGE system; Invitrogen) with morpholinepropanesulfonic acid running buffer as previously described (9). The gels were treated with 1 M salicylic acid and exposed to Kodak BioMax MR films at −80°C. For Western blotting, after electrophoresis, the proteins were transferred to polyvinylidene difluoride (PVDF) membrane, blocked with 5% nonfat dry milk in PBS, probed with a 1:2,000 dilution of monoclonal antibody (MAb) HS2 (anti-VP4) (34) or B4-2 (anti-NSP4) (36), and detected with a 1:5,000 dilution of peroxidase-labeled anti-mouse immunoglobulin G (IgG) (Chemicon). For expression of NSP4 in $NSP4^{219}$ siRNA-transfected cells, the cells were harvested at 12 hpi in lysis buffer (10 mM Tris-HCl [pH 7.5], 100 mM NaCl, 1 mM $CaCl_2$, 1% NP-40 [Sigma]), and 10 μg of protein was analyzed by Western blotting with MAb B4-2. $G_{M1}$ was detected with 0.2 μg/ml of the biotin-labeled B subunit of cholera toxin (Sigma) and 0.1 μg/ml of peroxidase-labeled streptavidin (Kirkegaard & Perry) as previously described (9). The chemiluminescence signal was generated with enhanced-chemiluminescence (ECL) Western blotting detection reagent (Amersham Pharmacia).

**siRNA transfection.** The sequences and characterization of the effect on rotavirus replication of the VP4 siRNA (named $siRNA^{VP4}$ in reference 10) and VP7 siRNA (named g9D in reference 43) used in this study have been previously reported (10, 43). To silence the expression of NSP4, a synthetic siRNA corresponding to nucleotides (nt) 219 to 239 ($NSP4^{219}$) of RRV gene 10 with the target mRNA sequence 5′AAACGUCAAAGUGUUCAUAUA-3′ was designed. Duplex siRNAs were purchased from Dharmacon Research, and siRNA transfection for all of the experiments was performed basically as described by Silvestri et al. (43). Briefly, MA104 cells in six-well plates were grown to 80% to 90% confluence, the cells were washed with serum-free medium, and a mixture of 71.5 pmol of siRNA and 9.5 μl of Lipofectamine 2000 (Invitrogen) in 500 μl of Opti-MEM (Invitrogen) was added to each well. After 4 to 5 h of incubation, 500 μl of M199-20% FBS was added to each well. The cells were incubated in this mixture, and after 12 to 14 h, the medium was replaced with fresh M199-10% FBS until infection. A previously described laminin A/C siRNA (10, 13) or Lipofectamine 2000 alone was used as a negative control.

**Viral yield and rotavirus titer determination.** The titer of the viral yield from mock- or siRNA-transfected-infected MA104 cells and the rotavirus infectivity in rafts were determined on MA104 cells grown in 96-well plates by focus-forming unit (FFU) assay as previously described (9). For measurement of virus yield, cells were frozen and thawed three times after 14 h of infection, the cellular debris was pelleted, and the infectious-virus titer in the supernatant was determined by FFU assay. For quantification of rotavirus infectivity in raft fractions, first the VP6 content in f4 from each condition was determined by enzyme-linked immunosorbent assay with anti-VP6 MAb 255/60 (17). The virus titer in an aliquot of each raft fraction containing the same amount of VP6 was determined on MA104 cells as described above.

**Electron microscopy.** Eighty to 90% confluent monolayers of MA104 cells grown in six-well plates were transfected with the indicated siRNA as described above. At 36 h posttransfection, the cells were infected with DXRRV at an MOI of 10. At 7 hpi, the cells were scraped from the plates, washed twice with PBS, fixed with 2.5% glutaraldehyde–0.1 M cacodylate buffer (pH 6.7), postfixed with 2% osmium tetroxide, dehydrated, and embedded in Epon resin. Ultrathin sections were double stained with 2% uranyl acetate and 1% lead citrate, mounted on copper grids, and observed at 80 kV under a Philips (Eindhoven, The Netherlands) model CM10 electron microscope. Image analysis was carried out with ImageJ software, version 1.34s (National Institutes of Health, Bethesda, Md.).

**Immunofluorescence and confocal microscopy.** MA104 cells were grown on BIOCOAT coverslips (Becton Dickinson) and infected with DXRRV at an MOI of 0.5. For some experiments, the cells were transfected with $NSP4^{219}$ siRNA as described above and 24 to 36 h posttransfection the cells were infected as indicated. At 11 hpi, the cells were fixed with 4% paraformaldehyde and permeabilized with 0.2% TX-100 as previously described (9). The cells were blocked with 10% goat serum and then stained for 1 h with the indicated antibodies. All

incubations and washes were performed at room temperature unless indicated otherwise; the fluorescently labeled secondary antibodies were incubated for 30 min. Protein disulfide isomerase (PDI) was stained with 1 μg/ml of anti-PDI (Stressgen) and anti-mouse–fluorescein isothiocyanate (FITC) (1 μg/ml; Southern Biotechnologies). To visualize the ERGIC, we labeled MAb G1/93 (Alexis Biochemical), which recognizes ERGIC-53, with Alexa-Fluor 488 (Molecular Probes). The *cis*-Golgi compartment was detected with polyclonal antibody GPP130 (Covance), and mitochondria were stained with an anti-pyruvate dehydrogenase E2/E3bp subunit MAb (Molecular Probes). After three washes of 5 min each, 1 μg/ml of anti-rabbit–FITC or anti-mouse–FITC, respectively (Southern Biotechnologies), was added. After staining, the cells were washed and VP4 or virion-assembled VP7 was detected with MAb HS2 (1:4,000) and biotin-labeled MAb 159 (159B; 1:500); bound antibodies were detected with 1 μg/ml of anti-mouse–Texas Red or streptavidin-Texas Red, respectively (Southern Biotechnologies). In some experiments, the nucleus was costained with a 1:20,000 dilution of TOTO-3 (Molecular Probes) in buffer containing 200 μg/ml of RNase A (QIAGEN) during the last antibody incubation to reduce the background from cytoplasmic RNA. In some experiments, double-labeled preparations were then incubated with a 1:10,000 dilution of our polyclonal rabbit anti-rotavirus R3 serum and Cy5-labeled anti-rabbit IgG (1 μg/ml; Abcam). After washing, the coverslips were air dried and mounted on a glass slide with AquaPoly/Mount (Polysciences, Inc.). Fluorescence was analyzed in an Eclipse TE300 confocal microscope (Nikon) and LaserSharp MRC-1024 software (Bio-Rad). Double staining was analyzed with the 488- to 568-nm band of an argon-krypton laser.

## RESULTS

**Rotavirus associates with rafts in MA104 cells.** Our experimental approach to address the role of VP4, VP7, and NSP4 in the targeting of rotavirus particles to the raft compartment was to inhibit the expression of these viral proteins by RNAi and look at the subsequent association of rotavirus proteins with the raft fraction (f4) in infected cells. We focused our studies on outer capsid proteins VP4 and VP7 and nonstructural ER receptor protein NSP4 because these three proteins had the highest likelihood of being directly involved in rotavirus particle interactions with rafts due to either their location on the virion or to their role during morphogenesis. It is known that polarized Caco-2 cells display morphological characteristics and functional similarities to enterocytes (50). Because of this, these cells have been an excellent in vitro model for studying rotavirus cell tropism and polarized release (5, 9, 21, 23). However, the transfection efficiency of these cells after differentiation and polarization is very low (data not shown; 6, 47) and this technical constraint made them unsuitable for our purposes. In contrast, the monkey kidney cell line MA104 displays transfection efficiencies of 75 to 90% (data not shown; 10, 43) and has been a useful model to study the effect of RNAi on rotavirus replication. In addition, studies have demonstrated that MA104 cells, like Caco-2 cells, undergo polarized release of virus during infection (20, 38). Therefore, we first investigated if rotavirus particles associate with lipid rafts in MA104 cells during infection as they do in Caco-2 cells. DXRRV-infected MA104 cells were metabolically labeled for 30 min and after 1 h in chasing medium, rafts were extracted by insolubility in cold TX-100, further separated by equilibrium centrifugation in OptiPrep density gradients, and analyzed by gel electrophoresis as described before (9). Similarly to what was observed in Caco-2 cells, the majority of the labeled viral proteins were solubilized by TX-100 (Fig. 1A, bottom fractions). However, a substantial portion of rotavirus structural proteins VP2, VP4, VP6, and VP7 and nonstructural protein NSP4 was enriched in f4 with respect to the neighboring fractions. In addition, in accordance with previous reports, an enrichment of dsRNA was also found in the raft fraction (data not shown; 9). The partially glycosylated forms of VP7 and NSP4, as well as dimers of this nonstructural protein (arrow in Fig. 1A), were also present in f4. The presence of the dimeric form of NSP4 was confirmed by Western blotting with MAb B4-2 (data not shown). To confirm that lipid rafts are enriched in f4, we checked for the presence of $G_{M1}$, a lipid that is enriched in these microdomains. For this purpose, we detected $G_{M1}$ by using its natural ligand, the B subunit of cholera toxin, by Western blotting (9, 45). As expected, we found $G_{M1}$ enriched in the low-density fractions of the OptiPrep gradient from rotavirus-infected cells. This finding, together with the insolubility and flotation indications, demonstrates that f4 corresponds to the raft fraction in MA104 cells, as it does in Caco-2 cells (Fig. 1B). These observations also suggest that the migration of rotavirus particles into rafts is a conserved process present in at least two different polarized cell lines.

**An siRNA corresponding to nt 219 to 239 ($NSP4^{219}$) of RRV gene 10 greatly reduces the synthesis of NSP4.** Small duplex siRNAs corresponding to the sequences of gene 4, gene 9, and gene 10 of DXRRV were synthesized (Dharmacon Research) and transfected into MA104 cells to study the role of the outer capsid proteins and NSP4 in rotavirus-raft association. We first evaluated the abilities of VP4, VP7, and $NSP4^{219}$ siRNAs to inhibit the synthesis of target protein and block rotavirus replication. MA104 cells were transfected with the different siRNAs and 24 h later infected with DXRRV. Virus yield and protein expression were determined as described in Materials and Methods. $NSP4^{219}$ is a potent inhibitor of rotavirus replication since the virus yield in cells transfected with this siRNA was reduced by 92% compared to controls (Fig. 1C). Similar levels of inhibition were reported when the expression of NSP4 was blocked with an siRNA that binds its mRNA at positions 183 to 203 (26).Transfection with eitherVP4 siRNA or VP7 siRNA also decreased the yield of viral progeny approximately 70% with respect to the controls (Fig. 1C), as previously described (10, 43). Western blot analysis of NSP4 in cells transfected with the three different siRNAs showed that $NSP4^{219}$ was very efficient at blocking the synthesis of NSP4 (Fig. 1D), and as expected, neither VP4 siRNA nor VP7 siRNA had an effect on the synthesis of NSP4. As previously described, the VP4 and VP7 siRNAs also inhibited the expression of the cognate proteins (data not shown; 10, 43). Together, these results show that siRNA homologous to the NSP4 gene sequence between nt 219 and 239 substantially reduces the synthesis of NSP4 and inhibits the production of viral progeny.

**Rotavirus-raft association is differentially affected by siRNAs.** The preceding results indicate that rotavirus proteins associate with rafts in MA104 cells and that siRNAs that target mRNAs of VP4, VP7, or NSP4 efficiently block the expression of their target proteins in MA104 cells and reduce viral yield. To test the effects of these three siRNAs on rotavirus-raft interactions, cell monolayers were transfected with VP4, VP7, $NSP4^{219}$, or laminin A/C siRNA. At 36 h posttransfection, the cells were infected with DXRRV, and 8 h later the cells were metabolically labeled and rafts were purified as described in Materials and Methods. As a positive control, we treated cells with 10 mM mβcdx since in Caco-2 cells cholesterol depletion with mβcdx interferes with the association of rotavirus particles with rafts (9). As expected, cholesterol sequestration signifi-

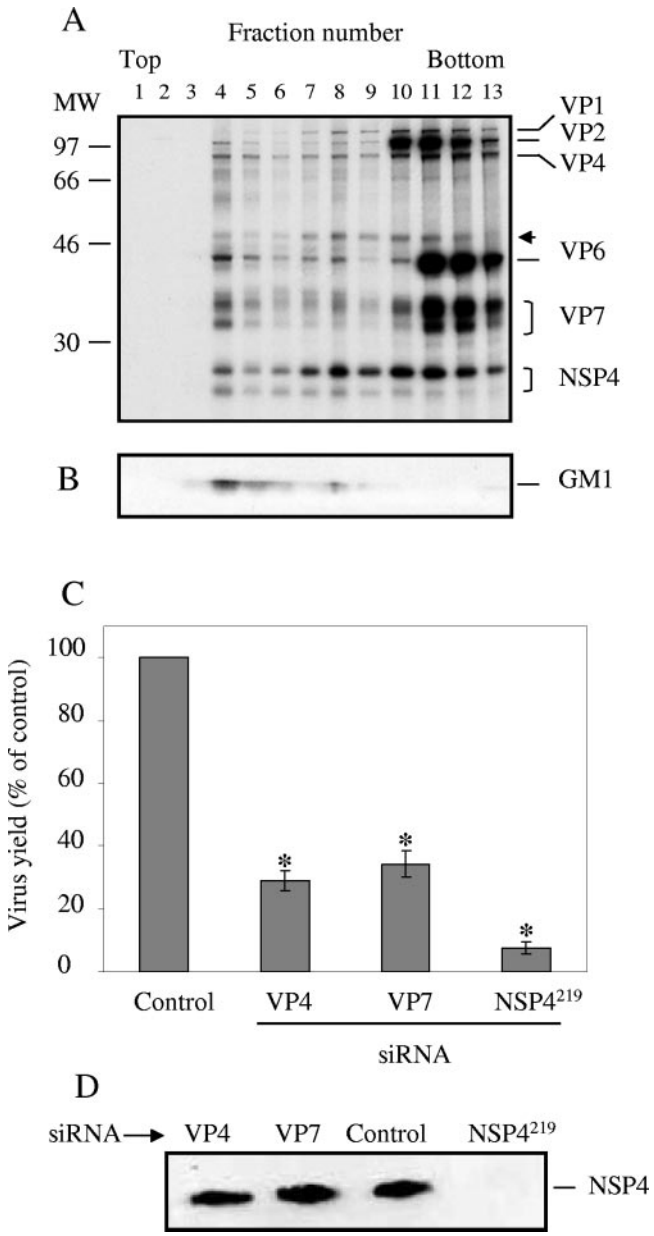


FIG. 1. Isolation of rafts and effects of siRNAs on rotavirus-infected MA104 cells. (A) Pulse-labeled rotavirus proteins associate with rafts in MA104 cells. MA104 cells were infected with DXRRV (MOI of 10) and metabolically labeled as described in Materials and Methods. After lysis in cold 1% TX-100, rafts were purified by equilibrium centrifugation in OptiPrep gradients, fractionated, and analyzed by SDS-PAGE and fluorography. The arrow indicates the migration of the dimeric form of NSP4. (B) Detection of $G_{M1}$ by Western blotting. Fractions from panel A were subjected to electrophoresis and transferred to PVDF membrane, the membrane was incubated with the biotinylated B subunit of cholera toxin and peroxidase-labeled streptavidin, and a signal was developed by ECL. (C) Effect of siRNAs on rotavirus yield. MA104 cells were transfected with 71.5 pmol of the indicated siRNA, and at 24 h posttransfection, the cells were infected for 14 h with DXRRV at an MOI of 1. The titer of the viral yield was determined on MA104 cells by FFU assay. Titers are expressed as percentages of the virus yield, where 100% represents the titer of virus grown in control transfected cells. Values are means from three experiments, and the standard error is indicated. *, $P < 0.05$ (one-sample *t* test). (D) Detection of NSP4 by immunoblotting in the presence of the indicated siRNA. MA104 cells were transfected and infected as described for panel C, and at 12 hpi they were lysed in 1% NP-40 lysis buffer and 10 μg of protein was separated by SDS-PAGE. Electrophoresed proteins were transferred to PVDF membrane, and the membrane was blocked and incubated with MAb B4-2. Bound antibody was detected with peroxidase-labeled anti-mouse IgG and ECL. MW, molecular weight marker (in thousands).

cantly reduced the floatation of rotavirus particles in the raft-containing fraction (Fig. 2A, βcdx lane). Similarly, the amount of rotavirus proteins present in the raft fraction was significantly reduced in cells that were transfected with the VP4 siRNA (Fig. 2A, VP4 lane) compared to the mock- and laminin A/C siRNA-transfected cells, suggesting that particles lacking VP4 are not efficiently targeted to cellular rafts. In contrast, VP7 siRNA was not effective at inhibiting the migration of viral proteins into f4 (Fig. 2A, VP7 lane). Interestingly, while the amount of VP7 in f4 was reduced more than threefold compared to the control in cells transfected with VP7 siRNA (Fig. 2A, compare VP7 lane with mock and laminin A/C lanes), the amount of the other viral proteins in f4 remained almost constant, suggesting that particles lacking VP7 were able to associate with rafts. When the effect of NSP4 siRNA$^{219}$ on targeting rotavirus particles to rafts was evaluated, we found that unlike VP7 siRNA, it reduced the association of rotavirus particles with rafts, suggesting a role for NSP4 in rotavirus particle-raft association (Fig. 2A, NSP4 lane). Lipofectamine alone and a rotavirus-unrelated siRNA had no effect on the partitioning of viral proteins into these lipid microdomains (Fig. 2A, mock and laminin A/C lanes). Since we did not find any difference between mock-transfected cells (Lipofectamine alone) and laminin A/C-transfected cells, for the following experiments only the results with mock-transfected cells are shown. Quantitation by densitometry of the percentage of viral proteins VP2, VP4, VP6, VP7, and NSP4 in f4 from three independent experiments showed that silencing of the synthesis of VP4, VP7, and NSP4 reduced the migration of rotavirus proteins into rafts by 64%, 14%, and 44%, respectively (Fig. 2B). Of note, independent quantitation of individual viral proteins in f4 confirmed that VP4 and NSP4$^{219}$ siRNAs, but not VP7 siRNA, altered the migration of rotavirus particles into rafts (data not shown).

In a previous study, we demonstrated that viral infectious particles, and not just soluble, unassembled proteins, migrated into the insoluble raft-containing component of the gradient (9). To determine if the $^{35}$S-labeled proteins migrating in f4 (Fig. 1A and 2A) were assembled into virions, we measured viral infectivity. For this purpose, the amount of viral particles present in f4 from VP4, VP7, and NSP4$^{219}$ siRNA-transfected or control transfected cells was normalized to VP6 content, an aliquot was diluted in M199 and activated with trypsin, and the virus titer was determined (8). Viral infectivity was found associated with rafts ($7.1 \times 10^7$ FFU/ml in control transfected cells) and was reduced by 72% and 87% when the synthesis of VP4 or NSP4 was blocked with the corresponding siRNA (Fig. 2C). In accordance with the results observed in Fig. 2B, silencing of VP7 slightly reduced viral infectivity in f4 by 40% with respect to the control (Fig. 2C). When we evaluated the presence of genomic dsRNA in the raft fraction from cells treated

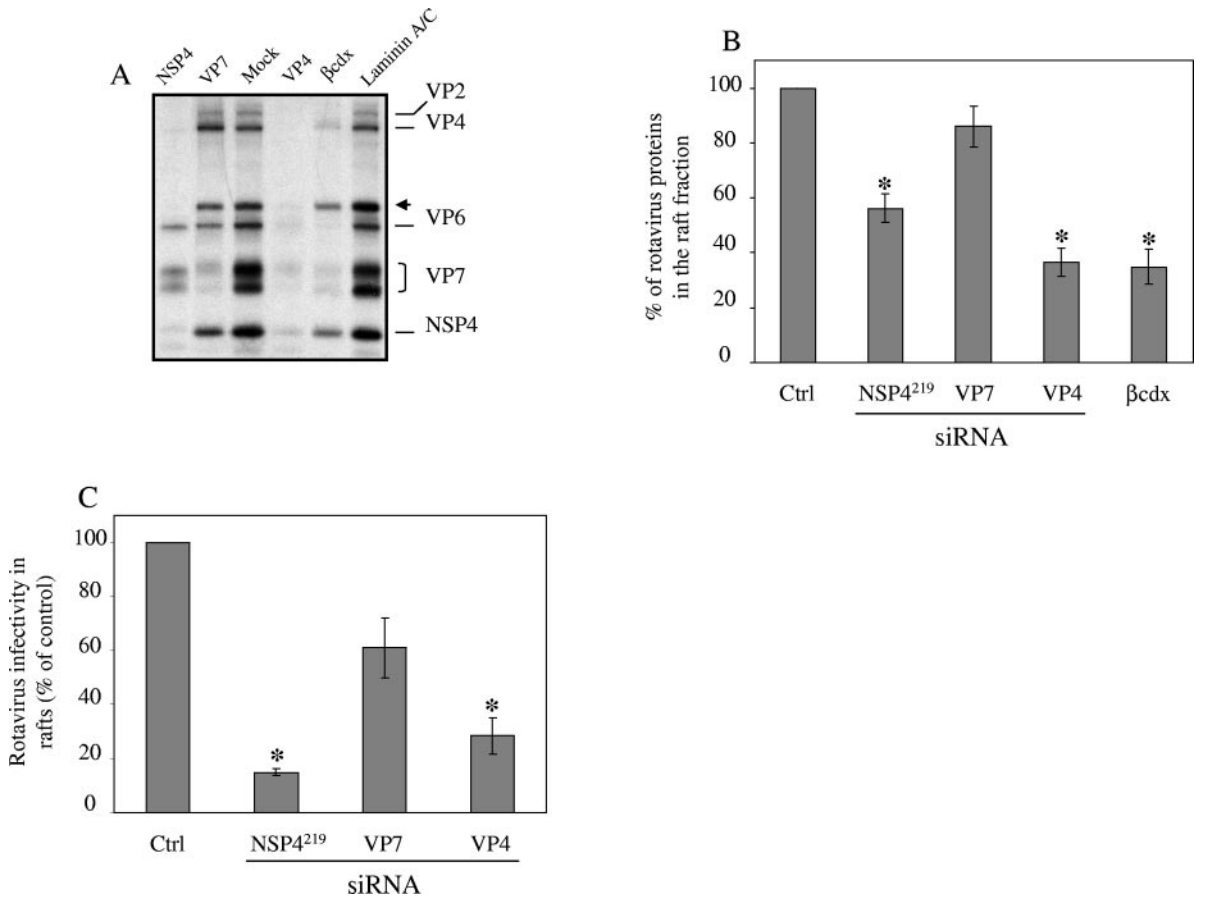


FIG. 2. Rotavirus-raft association is differentially affected by siRNAs. (A) MA104 cells were mock transfected or transfected with the siRNAs that silence the expression of the indicated protein. AT 36 h posttransfection, the cells were infected with DXRRV (MOI, 10) and pulse-labeled as described for Fig. 1A, and rafts were purified by OptiPrep density gradients. After fractionation, 250 μg of $^{35}$S-labeled protein of the raft fractions was analyzed by SDS-PAGE and fluorography. For an mβcdx control, 10 mM mβcdx was added to infected cells during starvation and maintained until the end of the experiment. One gel representative of at least three experiments is shown, and the migration of the viral structural proteins and NSP4 is indicated, including the dimeric form of NSP4 (arrow). (B) Densitometric analysis of rotavirus proteins in f4. The radioactive signal for rotavirus proteins VP2, VP4, VP6, VP7, and NSP4 in f4 from gels like the one shown in panel A was quantified with the ChemiImager 4400 low-light imaging system (Alpha Innotech Corp.). Results are expressed as the percentage of these proteins in the raft fraction, where 100% represents the overall amount of these proteins in control transfected cells. (C) Rotavirus infectivity in the raft fraction. Raft fractions from MA104 cells infected with DXRRV and transfected with the indicated siRNAs were normalized to VP6 content by enzyme-linked immunosorbent assay, and virus titers were determined on MA104 cells by FFU assay. Results are expressed as the percentage of infectivity in f4, where 100% represents the infectivity in control lipofected cells. Values are means ± standard errors from at least three experiments. *, $P < 0.05$ (one-sample $t$ test). Ctrl, control.

with the different siRNAs, we found that the amount of dsRNA in each fraction correlated with the amount of viral proteins and infectivity shown in Fig. 2 (data not shown). Together, these results show that siRNA-mediated depletion of VP4 and NSP4, but not VP7, substantially reduce the association of rotavirus particles with rafts.

**NSP4 indirectly contributes to the association of rotavirus particles with rafts.** The inhibition of the partitioning of viral proteins into lipid microdomains in cells transfected with NSP4$^{219}$ siRNA could be caused by (i) an indirect contribution of NSP4 to rotavirus particle-raft association during either transport or maturation of the virus in the ER or (ii) the lack of particles available for transit. In order to elucidate the role of NSP4 in this association, we looked at the effect of glycosylation inhibition in the presence of TM on rotavirus particle-raft interaction and checked for the cellular localization of rotavirus particles in the absence of NSP4 by double indirect immunofluorescence staining and confocal microscopy. For the TM experiment, monolayers of MA104 cells were infected and treated with TM as described in Materials and Methods. Lipid rafts were then purified, and the fractionated gradients were analyzed by SDS-PAGE. TM treatment prevented the glycosylation of VP7 and NSP4, as indicated by the appearance of their unglycosylated protein precursors (Fig. 3B). In addition to the blockage of glycosylation, the dimeric form of NSP4 is also affected by TM, as the band migrating above VP6 (arrow in Fig. 3A) disappeared in cells treated with TM (Fig. 3B), suggesting that glycosylation is a prerequisite for dimer formation. Of note, only small amounts of rotavirus proteins were found floating in the detergent-resistant fraction in the presence of TM (compare f4 in Fig. 3A and B), and as expected (11), the rotavirus infectivity in this fraction was reduced by

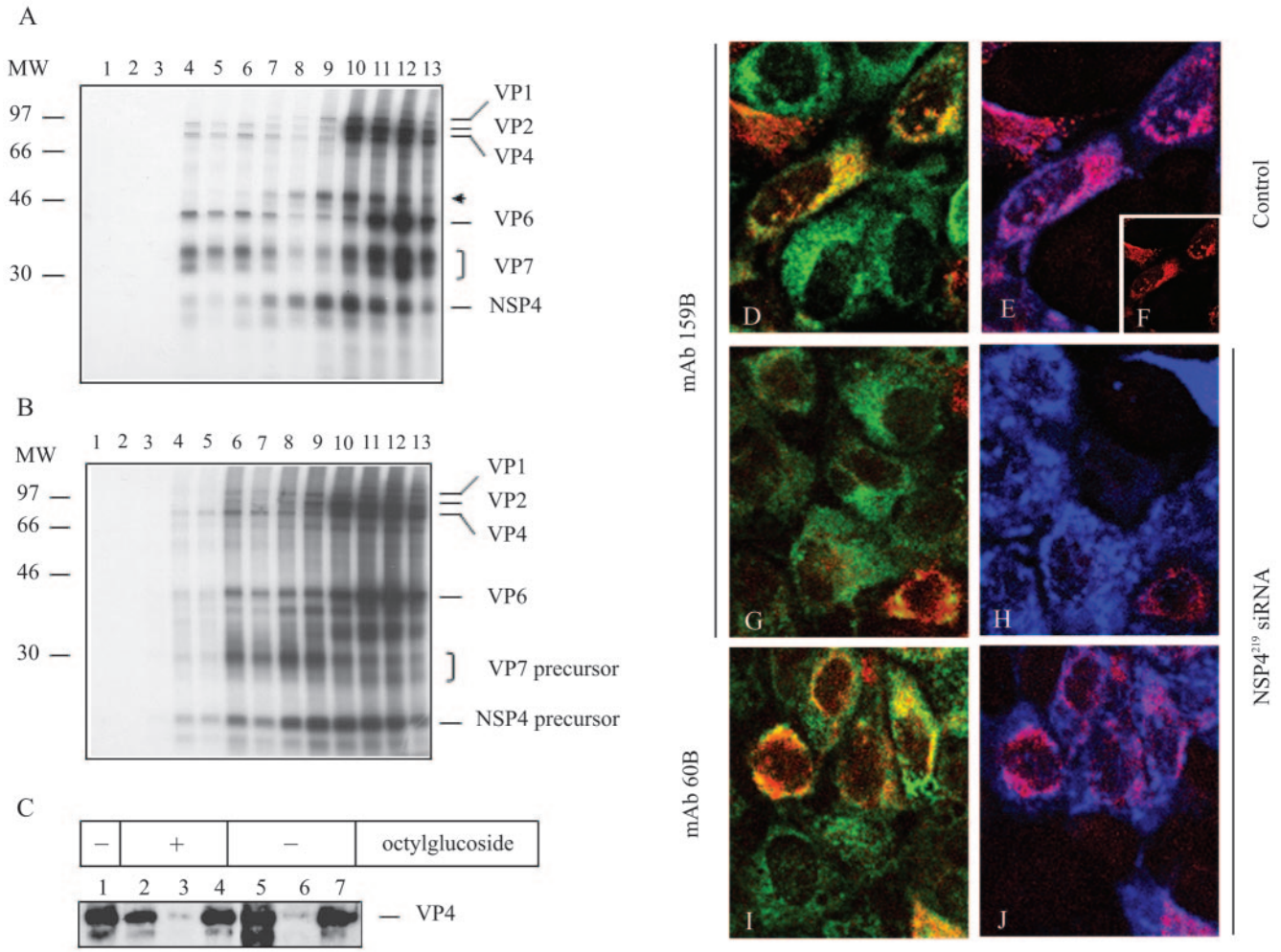


FIG. 3. Role of NSP4 in targeting of virions and VP4 to rafts. (A and B) TM treatment prevents the association of rotavirus particles with rafts. Rafts were purified from untreated (A) or TM-treated (B), DXRRV-infected MA104 cells as described in Materials and Methods. OptiPrep density gradients were fractionated and analyzed by SDS-PAGE and fluorography. TM treatment (10 μg/ml) started at 6 hpi and continued to the end of the experiment (B). The positions of viral proteins are indicated at the right, including unglycosylated precursors of VP7 and NSP4 (B) and the dimeric (arrow) form of NSP4 (A). A set of gels representative of at least three experiments is shown. (C) Most of the VP4 associated with rafts comes from viral particles. MA104 cells were infected with DXRRV at an MOI of 10, and at 9 hpi, rafts were purified by cold 1% TX-100 extraction and OptiPrep gradient centrifugation. The rotavirus particles present in the isolated raft fraction were pelleted by ultracentrifugation, and the PUSN was concentrated in a Centriplus YM-10 unit. The presence of VP4 in the pellet (lanes 2 and 5), supernatant (lanes 3 and 6), and semipurified TLPs (lanes 4 and 7) was detected by SDS-PAGE and immunoblotting with MAb HS2. Before ultracentrifugation, aliquots of f4 (lanes 2 and 3) or semipurified TLPs (lane 4) were adjusted to 60 mM octylglucoside, incubated for 30 min at 37°C (lanes 2 to 4), and subjected to ultracentrifugation as described above. Lane 1 represents an aliquot of the starting f4. (D to J) Virion-assembled VP7 colocalizes with PDI in control cells but not in NSP4$^{219}$ siRNA-transfected cells. MA104 cells grown on coverslips were mock transfected (D to F) or transfected with NSP4$^{219}$ siRNA (G to J), and at 24 h posttransfection, the cells were infected with DXRRV (MOI, 0.5) for 12 h. The cells were then fixed, permeabilized, and stained with anti-PDI and anti-mouse–FITC. After washing, rotavirus VP7 was detected with MAb 159B (D to H) or 60B (I and J). Bound antibodies were detected with streptavidin-Texas Red. The double-labeled preparations were then incubated with a 1:10,000 dilution of polyclonal rabbit serum (anti-rotavirus R3) and Cy5-labeled anti-rabbit IgG. The coverslips were mounted in glass slides and analyzed in an Eclipse TE300 confocal microscope (Nikon). The left part shows the distribution of PDI in green, and the colocalization with VP7 is shown in yellow. The signal of MAb 159B for panels D and E is shown in panel F. The right part shows the same field but colocalization of rotavirus antigen (R3 stained, blue signal) with VP7 (red signal). All images were obtained with a 60× objective and processed with Adobe Photoshop software. MW, molecular weight marker (in thousands).

92% in the presence of TM in comparison with control infected cells. We also analyzed the distribution of TLPs in the ER with MAb 159B (which primarily recognizes a conformation of VP7 found on assembled mature viral particles) (12) and an anti-PDI MAb as an ER marker (16). In control or NSP4$^{219}$ siRNA-transfected cells, localization of PDI followed the pattern of a continuous network with major abundance in the perinuclear region (green signal in Fig. 3D, G, and I). When we compared the distribution of virion-associated VP7 (red signal in Fig. 3D and E and insert in panel F) with that of PDI, we found that in the majority of infected cells these two markers colocalized (Fig. 3D). This in agreement with a previous report that showed that mature, virion-associated VP7 interacts with PDI (31). In contrast, in NSP4$^{219}$ siRNA-trans-

fected cells we could not find TLPs inside the ER, as indicated by the lack of red staining with MAb 159B in transfected cells (Fig. 3G). Note that a couple of cells in Fig. 3G and H do demonstrate virion-associated VP7 in the ER (red cells in Fig. 3G and H); however, since the transfection efficiency is not 100%, these cells presumably were not transfected with $NSP4^{219}$ siRNA. The lack of staining with MAb159B was not due to the lack of infection since all cells were positive for rotavirus antigen when immunostained with a polyclonal anti-rotavirus serum (blue signal in Fig. 3E, H, and J), nor was it due to the absence of VP7 since we found positive staining for VP7 with biotin-labeled MAb 60 (60B), which primarily recognizes a non-virion-associated form of VP7 (Fig. 3I and J). These results support the hypothesis that the contribution of NSP4 to rotavirus-raft association involves particle assembly or maturation of the virus in the ER.

**VP4 association with rafts is primarily due to incorporation into viral particles in the ER.** Close examination of Fig. 2A (NSP4 lane) and 3B reveals that when the amount of NSP4 was decreased by either $NSP4^{219}$ siRNA or TM treatment, the amount of VP4 in the raft fraction was also reduced. When we measured the radioactive signal of VP4 over the 13 fractions of the gradient by densitometry, we found that there was a 43.5% reduction in VP4 in f4 in cells treated with TM in comparison with f4 from control cells. These observations suggested that the inhibition of rotavirus particle migration into lipid rafts also reduced the targeting of VP4 to these microdomains. In order to determine if particle assembly mediates targeting of VP4 to rafts, rafts were isolated from infected MA104 cells as described for Fig. 1. The purified f4 was then diluted, and rotavirus particles in rafts were pelleted by ultracentrifugation. The PUSN was concentrated, and the presence of VP4 in pelleted material and concentrated PUSN was detected by immunoblotting. To rule out the possibility that membrane aggregates in the raft fraction were trapping free VP4 during ultracentrifugation, half of the volume of the raft fraction was solubilized with 60 mM octylglucoside (4). As seen in Fig. 3C, both in the presence and in the absence of octylglucoside, very small amounts of non-virion-associated free VP4 could be recovered from the concentrated PUSN of the raft fraction (lanes 3 and 6 in Fig. 3C). In contrast, a ninefold enrichment of VP4 was detected in the pelleted material (lanes 2 and 5 in Fig. 3C). Since the treatment of semipurified virus with 60 mM octylglucoside does not solubilize VP4 from TLPs (lanes 4 and 7 in Fig. 3C), these results suggest that the most of the VP4 associated with rafts in MA104 cells is virion associated rather than soluble and likely comes from viral particles derived from the ER and not from a cytoplasmic source.

**Silencing the expression of VP4 results in accumulation of nonenveloped immature particles within the ER.** Our results showed that in the absence of VP4 the rotavirus virion does not migrate into the raft fraction. To further characterize the cellular location of particles lacking VP4 or VP7 or particles assembled in the absence of NSP4, we studied siRNA-transfected cells infected with rotavirus by transmission electron microscopy. As shown in Fig. 4, in mock-transfected cells, viroplasms were observed adjacent to the ER membrane with DLPs budding into the lumen of the ER. The presence of membrane-enveloped intermediate particles, as well as mature TLPs that had lost their envelope, is clearly visible within the dilated cisternae of the ER (filled arrow, upper left panel of Fig. 4). In $NSP4^{219}$ siRNA-transfected cells, however, viroplasms were observed free in the cytoplasm with DLPs present in the cytoplasm and not in the ER (open arrow, upper right panel of Fig. 4). These results correlate with our confocal microscopy observations, in which we did not find colocalization between mature particles and PDI in $NSP4^{219}$ siRNA-transfected cells (Fig. 3G) and with previous observations that suggest that the lack of NSP4 reduces the formation of viral particles (26). Interestingly, a lack of ER membranes in proximity to the viroplasms was a consistent observation in cells transfected with $NSP4^{219}$ siRNA (upper right panel of Fig. 4), suggesting that in the absence of NSP4, viroplasms cannot bind to the ER, causing more extensive "drifting" of viroplasms and DLPs in the cytoplasm of the infected cell. Transfection of cells with VP7 siRNA resulted in the accumulation of enveloped particles within the ER (filled arrowhead, bottom left panel of Fig. 4), suggesting that VP7 is required for proper removal of the transient envelope. An analogous phenotype has been reported when cells were transfected with a different siRNA that also inhibits the expression of VP7 (26) and when cells were treated with agents that disrupt the proper folding of VP7, such as TM (39), dithiothreitol (46), or calcium-blocking drugs like thapsigargin (29). In VP4 siRNA-transfected cells, DLPs budding normally from viroplasms into the ER were observed and a small amount of enveloped intermediates was seen inside the ER. Strikingly, there was an unusual accumulation of nonenveloped immature particles inside the distended ER in these cells (open arrowhead, bottom right panel of Fig. 4), and this accumulation was reproducibly found when VP4 expression was inhibited. The immature particles tightly aggregate together to form a lattice or paracrystalline array (bottom right panel of Fig. 4). It is hard to tell if VP7 is present in these particles, but a close examination of some particles inside the paracrystalline array showed an electron-dense core surrounded by a lighter zone, suggesting that VP7 was present.

**Rotavirus particles colocalize with the ER-Golgi intermediate compartment.** Rotavirus progeny are released in polarized cells by a nonconventional secretory pathway that bypasses the Golgi, and it has been proposed that during this nonlytic release the virus uses vesicular carriers to reach the apical cell surface (21). Since our studies indicate that both surface proteins of the mature virion appear to associate with particles in the ER, at the beginning of the secretory process, we began to analyze the progression of rotavirus proteins through the exocytic pathway. For this purpose, we performed double immunofluorescence staining of rotavirus proteins and proteins specific for certain cellular organelles along the secretory pathway. Rotavirus proteins were detected with MAbs HS2 and 159B, which recognize VP4 and virion-assembled VP7, respectively (12, 34). To visualize the ERGIC, we used MAb G1/93, which recognizes ERGIC-53 (41). The *cis*-Golgi compartment was detected with polyclonal antibody GPP130, and mitochondria were stained with an anti-pyruvate dehydrogenase E2/E3bp subunit MAb. To avoid cross-reactivity, we stained first for cellular markers and then for rotavirus proteins. In noninfected MA104 cells, the lectin ERGIC-53 exhibited a punctate staining that is typical for the ERGIC in tissue culture cells (41). When this organelle is seen at higher magnification, the distribution resembles vesicular or tubelike structures concentrated in the

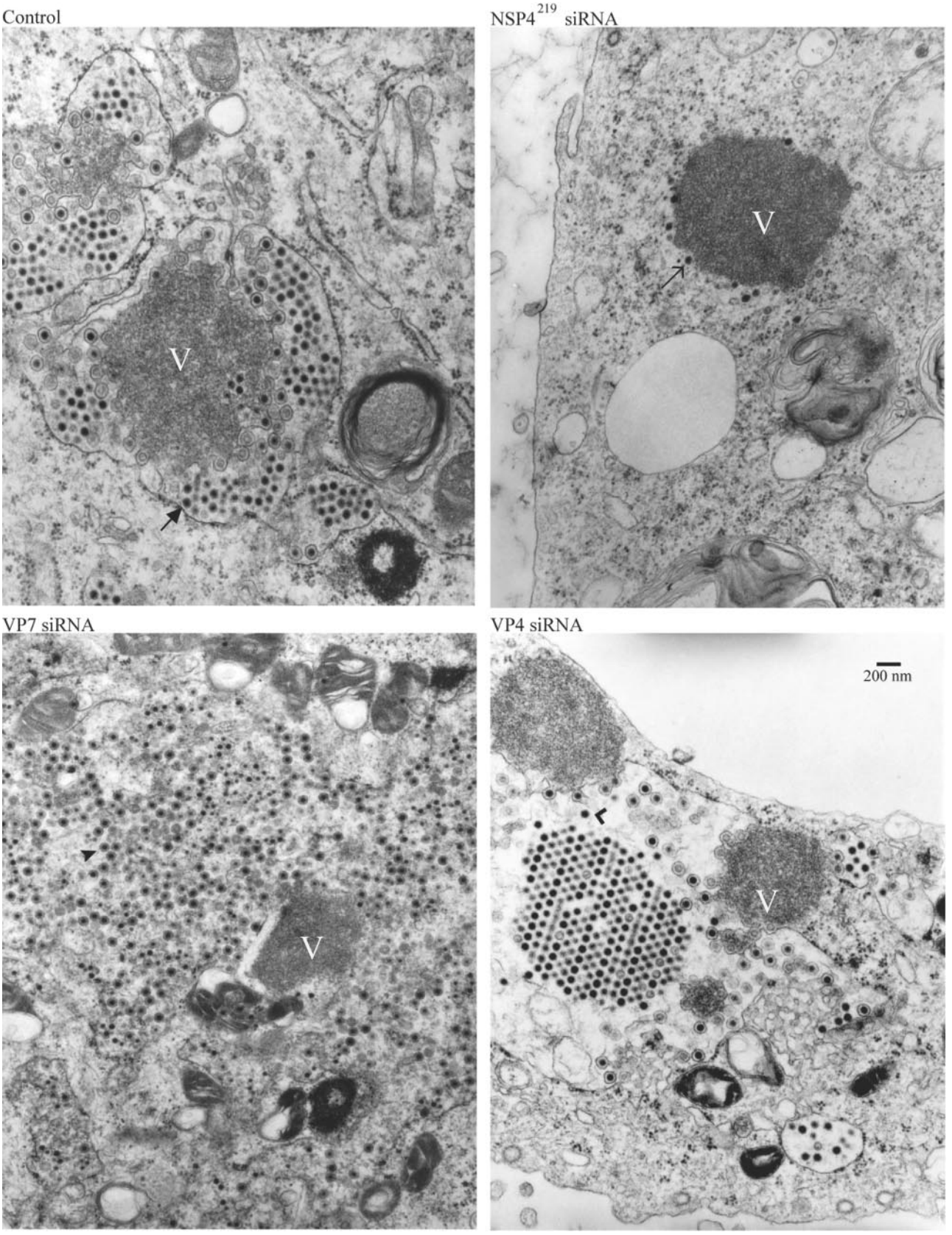


FIG. 4. Electron microscopy of MA104 cells transfected with different siRNAs. MA104 cells grown in six-well plates were control transfected or transfected with the indicated siRNA as described in Materials and Methods. At 36 h posttransfection, the cells were infected with DXRRV at an MOI of 10. After 7 h of infection, the cells were recovered, fixed in glutaraldehyde, and processed for transmission electron microscopy. V, viroplasm inclusions; filled arrow, TLPs inside the distended cisternae of the ER; open arrow, DLPs in the cytoplasm; filled arrowhead, enveloped intermediate particle inside the ER; open arrowhead, nonenveloped immature particle inside the ER next to the paracrystalline array.

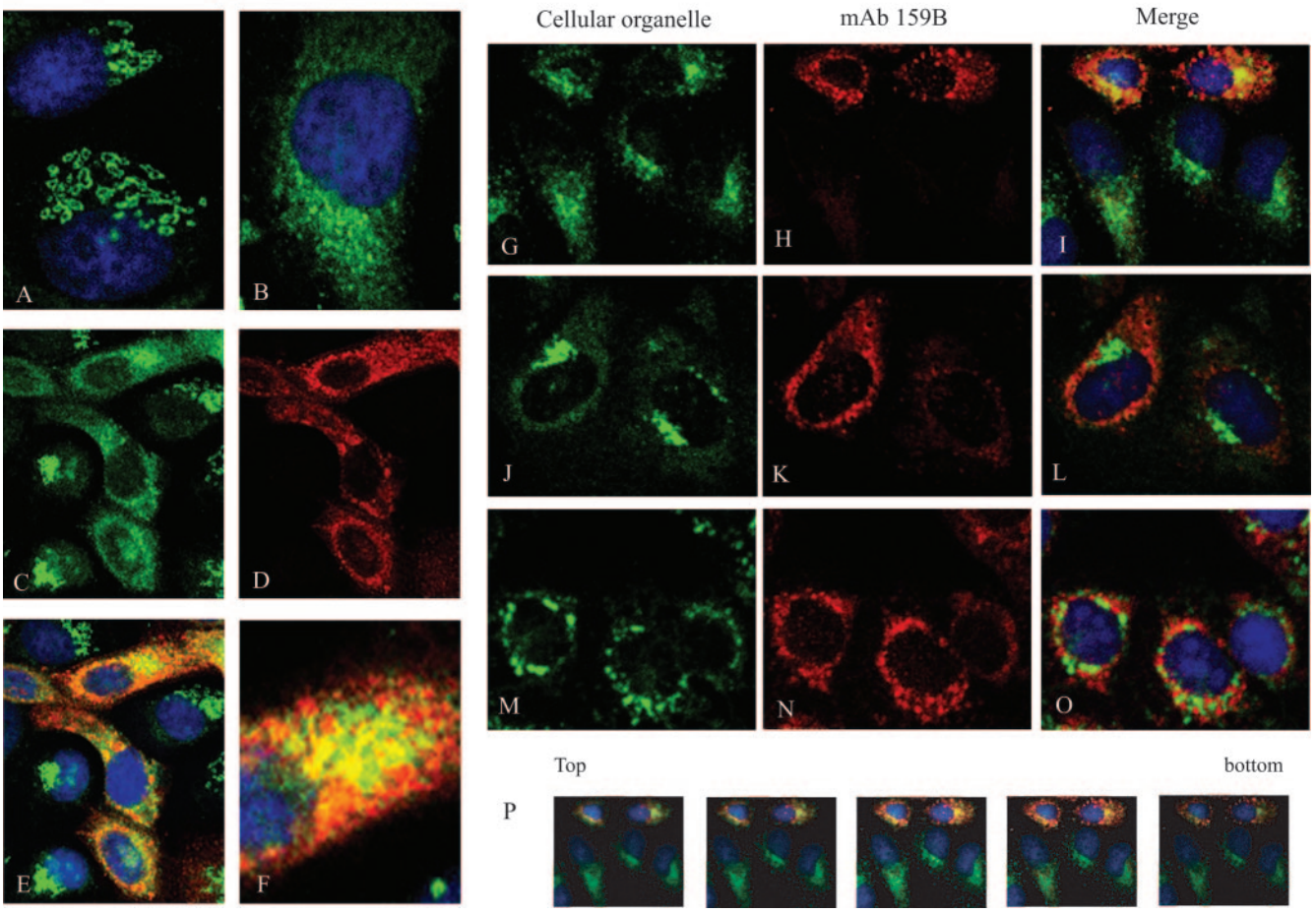


FIG. 5. Colocalization of ERGIC-53 and rotavirus proteins. MA104 cells grown on coverslips were not infected (A) or infected with DXRRV at an MOI of 0.5 (B to P), and at 12 hpi, cells were fixed and permeabilized and incubated with anti-G1/93 (A to I and P), anti-GPP130 (J to L), and anti-pyruvate dehydrogenase E2/E3bp subunit (M to O) antibodies as markers for the ERGIC, the *cis*-Golgi, or mitochondria, respectively. After washing, the appropriate secondary antibody was added and then the cells were stained for VP4 with MAb HS2 (C to F) or for virion-assembled VP7 with MAb 159B (G to P) as described in Materials and Methods. The nucleus was costained with a 1:20,000 dilution of TOTO-3, and the preparations were mounted and analyzed by confocal microscopy as described in the legend to Fig. 3. In all images, the green signal shows the distribution of a cellular organelle and the red signal shows the distribution of rotavirus proteins. (P) Representative sequential sections with a thickness of 1 μm acquired from the bottom to the top of panel I. All images were obtained with a 60× objective; panels A, B, and F show a 2× zoom image. The digital images were processed with Adobe Photoshop.

juxtanuclear region (Fig. 5A). In DXRRV-infected cells, a clear change in the distribution of ERGIC-53 was observed; the tubovesicular structures were lost, and a more diffuse staining of ERGIC-53 over the entire cytoplasm was observed (Fig. 5B and C). When VP4 was costained in infected cells (Fig. 5D), a small but readily detectable fraction of ERGIC-53 colocalized with this viral protein (Fig. 5E) and this colocalization was more prominent in areas where ERGIC-53 was concentrated (Fig. 5F). To determine if TLPs also colocalize with ERGIC-53, we used MAb 159B. Like VP4, mature VP7 partially colocalizes with the lectin ERGIC-53 and this colocalization is also concentrated in the regions where ERGIC-53 most accumulates (Fig. 5I). The localization of ERGIC-53 and rotavirus particles in the same confocal plane was confirmed by a stack of optical sections with a thickness of 1 μm (Fig. 5P). As predicted from prior studies (21), we could not find colocalization of either *cis*-Golgi (Fig. 5J to L) or mitochondrial markers with rotavirus particles (Fig. 5M to O), confirming that rotavirus particles do not associate with these organelles during maturation and secretion.

## DISCUSSION

In this work, we inhibited the expression of rotavirus outer capsid proteins VP4 and VP7 and nonstructural protein NSP4 in order to understand their role in the targeting of rotavirus particles to the raft compartment during secretion from the cell. We have shown that silencing of VP4 reduces the association of rotavirus particles with rafts and that inhibition of the synthesis of VP7 does not have a drastic effect on the migration of virions into rafts. At first glance, we could attribute the reduction of viral proteins in rafts in siRNA-transfected cells to the absence of viral particles; however, this seems not to be the case because the assembly of particles lacking either VP4 or

VP7 has been previously reported (10, 26, 43) and because we found that the amount of these particles in the soluble fractions of the OptiPrep gradient was the same under both conditions (data not shown). Since both VP4 and VP7 siRNAs are equally efficient at shutting down the expression of their target proteins but only VP4 siRNA blocks the migration of particles into rafts, we conclude that VP4, but not VP7, plays a direct role in the association of virus with rafts. We also described a new siRNA that was able to block the synthesis of NSP4 and to substantially reduce viral replication. We hypothesized that after NSP4 inhibition by $NSP4^{219}$ siRNA, we would not be able to detect an association of rotavirus particles with rafts because of several reasons. First, it was already known that NSP4 functions as an intracellular receptor that binds VP6 and facilitates the budding of DLPs into the ER; second, glycosylation of this nonstructural protein is required for removal of the lipid coat from the transient enveloped particle in the ER; and third, it had been recently shown that in the absence of NSP4, the assembly of DLPs and TLPs is greatly reduced (26). As predicted, $NSP4^{219}$ siRNA reduced the association of rotavirus particles with rafts and this reduction could be explained by an indirect contribution of NSP4 to the migration of rotavirus to rafts, involving either one of the steps in the exocytosis of the virion particle, i.e., transport or maturation of the virus in the ER, or by blocking the formation of DLPs, which is a step prior to entry into this organelle. Since previous studies have found that the effect of TM on NSP4 is not related to the reduction of the synthesis of this protein or to the production of viral particles, our TM data support the hypothesis of an indirect contribution of NSP4 to rotavirus-raft association by blocking the transit of particles in the ER.

While examining the role of NSP4 in rotavirus-raft association, we found that inhibition of rotavirus migration into these lipid microdomains by either siRNAs or TM treatment also blocked the targeting of VP4 to rafts. This observation was surprising since Delmas et al. recently showed that although inhibition of glycosylation with TM in Caco-2 cells reduced the amount of mature viral particles associated with rafts, it did not interfere with the targeting of VP4 to these microdomains (11). Technical differences such as the cell line and stage of differentiation of the cells may account for this apparent discrepancy, since it is known that functional differences exist between MA104 cells and highly polarized Caco-2 cells (5). On the other hand, the fact that the reduction of VP4 in the raft fraction of TM-treated cells is not proportional to the reduction of the other viral proteins (compare f4 in Fig. 3A and B) may indicate the presence of two populations of VP4, one that is independently targeted to rafts and whose association is not affected by TM or the absence of NSP4, and a second, larger pool of VP4 whose association with rafts is mediated by particle formation in the ER. The concept of dual compartmentalization of rotavirus surface proteins is not new since it was shown that VP7 also exists in two forms; a membrane-associated form and a virus-associated one (22). In order to determine if two populations of VP4 coexist in rafts, we separated VP4-containing rotavirus particles from non-virion-associated VP4 in the raft fraction by ultracentrifugation and showed that most, but not all, of the VP4 in rafts is found in particles probably assembled in the late stages of transit through the ER. If VP4 is crucial for the association of rotavirus particles with rafts and the assembly of this protein into the viral particle takes place at a late stage of viral morphogenesis in the ER, we would expect an accumulation of viral particles in the ER in the absence of VP4. This hypothesis is supported by our electron microscopy observations, in which we found that the silencing of VP4 during rotavirus assembly directs virions to a close packaging of the particles in paracrystalline arrays. Our proposed interpretation of these ultrastructural findings is that, in the absence of VP4, the carbohydrate moieties on the surface of VP7 bind the particles together, leading to the formation of these arrays and consequently the aggregation of particles in the ER. Recently Déctor et al. showed the presence of enveloped and nonenveloped particles inside the ER in VP4 siRNA-transfected cells, but those authors did not find the paracrystalline array of particles reported in this work (10), possibly because at early times postinfection a higher MOI is needed to reach a critical concentration of particles inside the ER that promotes this paracrystalline arrangement. This observation and the purification of spikeless TLPs by cesium chloride gradients led those authors to conclude that VP4 is essential for neither assembly nor release of DLPs from the ER. However, purification of the spikeless particles recovered from VP4 siRNA-transfected cells in the study by Déctor et al. was performed at 18 hpi, which in MA104 cells likely reflects release of viral progeny by cellular lysis. In any case, our observations extend their findings and support the idea that in order to leave the ER via a nonlytic mechanism, TLPs require VP4. In this regard, the recent characterization of rotavirus membrane enveloped viral intermediates from infected MA104 cells showed that these contain VP4, VP7, and NSP4 and that even after detergent extraction, VP4 remained attached to the DLP (M. Zayas, M. Camacho, T. López, C. F. Arias, and S. López, Abstr. Int. Meet. Virol., abstr. V-386, 2005). Moreover, Trask and Dormitzer recently reported that in order to reconstitute infectious TLPs from noninfectious DLPs and purified recombinant VP4 and VP7, assembly of VP4 onto the recoated particle has to take place before the assembly of VP7 (P. Dormitzer, personal communication). These findings support the idea that VP4 assembly into particles takes place inside or in the vicinity of the ER and not at a later time point in the exocytic pathway when VP4 is added to VP7-coated particles. Several lines of evidence suggest a clear participation of the ER in targeting proteins to rafts. First, TX-100-resistant membranes have been detected in isolated membranes from the ER (42); second, ER proteins have been identified associated with lipid rafts in T cells and monocytes (25, 48); and finally, recent findings have shown that in mammalian cells the commitment of components of glycolipid-enriched membranes to enter these microdomains takes place inside the ER (37).

Increasing evidence suggests participation of the intermediate compartment in rotavirus maturation. The differential sensitivity of NSP4 and VP7 to endoglycosidase H during brefeldin A treatment implies that VP7 maturation takes place in the ERGIC (32). Xu et al. found that NSP4 accumulates in this organelle when it is transfected into COS-7 cells (49), and Delmas et al. recently proposed that VP4 assembly occurs in a post-ER compartment (11). Finally our studies indicate that

both rotavirus surface proteins on the mature virion appear to associate with particles in the ER at the beginning of the secretory process. Given these observations, we decided to analyze the progression of rotavirus proteins through the exocytic pathway. We found that rotavirus infection significantly changes the distribution of ERGIC-53 from a juxtanuclear vesicle-like pattern to a more dispersed one. A change in the distribution of ERGIC-53 has been previously reported when NSP4 alone was transiently expressed in COS-7 cells (49); however, the redistribution of ERGIC-53 induced by NSP4 alone exhibited a pattern different from the one observed here, presumably due to the coexpression of other rotavirus proteins. The role of individual viral proteins in this ERGIC rearrangement is an important question that will be addressed in future studies. Since live-imaging microscopy and ultrastructural studies have shown that ERGIC-53 predominantly localizes near the *cis* side of the Golgi (3, 24) and we did not find any colocalization between gpp130 and mature virions, we propose that at some stage during maturation or release, rotavirus particles transit through an ERGIC-53-containing organelle, presumably the ER-Golgi intermediate compartment, but exit the traditional secretory pathway before the *cis*-Golgi. In this regard, the diffuse staining of ERGIC-53 observed during rotavirus infection resembles what is seen when cells are rewarmed to 37°C after exit from the ERGIC has been blocked by incubation at 15°C (24). Interestingly, these rewarming experiments suggested that the retrograde traffic from the ERGIC to the ER bypasses the Golgi apparatus. Since nonlytically released rotavirus also bypasses the Golgi, one might speculate that during this retrograde traffic, the virus and ERGIC-53 colocalize to the same vesicles or organelle. Nevertheless, due to the constant recycling of ERGIC-53 between the ER and the ERGIC, we cannot rule out the possibility that some of the colocalization observed between VP4 or VP7 and ERGIC-53 actually occurs in the budding structures of the ER where ERGIC-53 concentrates (2, 24, 41).

It is generally accepted that in the secretory pathway, newly synthesized exocytic proteins leave the ER in COPII vesicles at the transitional elements of the rough ER and migrate to the Golgi apparatus through the ERGIC (1, 2, 24). However, during the last decade, intensive research in the area of cellular trafficking has shown the existence of new routes of transport. Endosomal recycling, plasma membrane transporters, membrane flip-flop, and membrane blebbing are now generally accepted as alternative exocytic mechanisms (33). The likely presence of rotavirus particles in the ERGIC raises several interesting questions to be addressed in future studies. Does the virus follow an as-yet-undescribed route from the ER to the ERGIC to the plasma membrane, and if so, do any cellular proteins also use this pathway? Is virus traveling to the cell membrane carried in vesicles? If so, what types of vesicles are involved? How and where does the virus-raft association take place? Blocking the recycling of ERGIC-53 either in the ER or in the ERGIC by different biochemical or thermal manipulations, as well as costaining of transport vesicle markers and viral proteins, should help clarify which transport pathways are directly involved in rotavirus maturation and release.

## ACKNOWLEDGMENTS

This work was supported by a VA merit review grant and by NIH grants R01AI21362 and DK56339-05.

We thank Shi-Qiang Qiu and Andrew Wieczorek for technical assistance. We specially thank Maria C. Jaimes, Martijn Fenaux, Ningguo Feng, and Ferdinando Liprandi for useful discussion.

## REFERENCES

1. **Aridor, M., S. I. Bannykh, T. Rowe, and W. E. Balch.** 1995. Sequential coupling between COPII and COPI vesicle coats in endoplasmic reticulum to Golgi transport. J. Cell Biol. **131:**875–893.
2. **Bannykh, S. I., T. Rowe, and W. E. Balch.** 1996. The organization of endoplasmic reticulum export complexes. J. Cell Biol. **135:**19–35.
3. **Ben-Tekaya, H., K. Miura, R. Pepperkok, and H. P. Hauri.** 2005. Live imaging of bidirectional traffic from the ERGIC. J. Cell Sci. **118:**357–367.
4. **Brown, D. A., and J. K. Rose.** 1992. Sorting of GPI-anchored proteins to glycolipid-enriched membrane subdomains during transport to the apical cell surface. Cell **68:**533–544.
5. **Ciarlet, M., S. E. Crawford, and M. K. Estes.** 2001. Differential infection of polarized epithelial cell lines by sialic acid-dependent and sialic acid-independent rotavirus strains. J. Virol. **75:**11834–11850.
6. **Cryan, S. A., and C. M. O'Driscoll.** 2003. Mechanistic studies on nonviral gene delivery to the intestine using in vitro differentiated cell culture models and an in vivo rat intestinal loop. Pharm. Res. **20:**569–575.
7. **Cuadras, M. A., C. F. Arias, and S. Lopez.** 1997. Rotaviruses induce an early membrane permeabilization of MA104 cells and do not require a low intracellular $Ca^{2+}$ concentration to initiate their replication cycle. J. Virol. **71:**9065–9074.
8. **Cuadras, M. A., D. A. Feigelstock, S. An, and H. B. Greenberg.** 2002. Gene expression pattern in Caco-2 cells following rotavirus infection. J. Virol. **76:**4467–4482.
9. **Cuadras, M. A., and H. B. Greenberg.** 2003. Rotavirus infectious particles use lipid rafts during replication for transport to the cell surface in vitro and in vivo. Virology **313:**308–321.
10. **Déctor, M. A., P. Romero, S. Lopez, and C. F. Arias.** 2002. Rotavirus gene silencing by small interfering RNAs. EMBO Rep. **3:**1175–1180.
11. **Delmas, O., A. M. Durand-Schneider, J. Cohen, O. Colard, and G. Trugnan.** 2004. Spike protein VP4 assembly with maturing rotavirus requires a postendoplasmic reticulum event in polarized Caco-2 cells. J. Virol. **78:**10987–10994.
12. **Dormitzer, P. R., D. Y. Ho, E. R. Mackow, E. S. Mocarski, and H. B. Greenberg.** 1992. Neutralizing epitopes on herpes simplex virus-1-expressed rotavirus VP7 are dependent on coexpression of other rotavirus proteins. Virology **187:**18–32.
13. **Elbashir, S. M., W. Lendeckel, and T. Tuschl.** 2001. RNA interference is mediated by 21- and 22-nucleotide RNAs. Genes Dev. **15:**188–200.
14. **Estes, M. K.** 2001. Rotaviruses and their replication, p. 1747–1785. *In* D. M. Knipe, P. M. Howley, D. E. Griffin, R. A. Lamb, M. A. Martin, B. Roizman, and S. E. Straus (ed.), Fields virology, 4th ed., vol. 2. Lippincott Williams & Wilkins, Philadelphia, Pa.
15. **Estes, M. K., and J. Cohen.** 1989. Rotavirus gene structure and function. Microbiol. Rev. **53:**410–449.
16. **Freedman, R. B., T. R. Hirst, and M. F. Tuite.** 1994. Protein disulphide isomerase: building bridges in protein folding. Trends Biochem. Sci. **19:**331–336.
17. **Greenberg, H., V. McAuliffe, J. Valdesuso, R. Wyatt, J. Flores, A. Kalica, Y. Hoshino, and N. Singh.** 1983. Serological analysis of the subgroup protein of rotavirus, using monoclonal antibodies. Infect. Immun. **39:**91–99.
18. **Hammond, C., and A. Helenius.** 1994. Quality control in the secretory pathway: retention of a misfolded viral membrane glycoprotein involves cyclin between the ER, intermediate compartment, and Golgi apparatus. J. Cell Biol. **126:**41–52.
19. **Hauri, H. P., F. Kappeler, H. Andersson, and C. Appenzeller.** 2000. ERGIC-53 and traffic in the secretory pathway. J. Cell Sci. **113**(Pt. 4)**:**587–596.
20. **Jones, L. V., R. W. Compans, A. R. Davis, T. J. Bos, and D. P. Nayak.** 1985. Surface expression of influenza virus neuraminidase, an amino-terminally anchored viral membrane glycoprotein, in polarized epithelial cells. Mol. Cell. Biol. **5:**2181–2189.
21. **Jourdan, N., M. Maurice, D. Delautier, A. M. Quero, A. L. Servin, and G. Trugnan.** 1997. Rotavirus is released from the apical surface of cultured human intestinal cells through nonconventional vesicular transport that bypasses the Golgi apparatus. J. Virol. **71:**8268–8278.
22. **Kabcenell, A. K., M. S. Poruchynsky, A. R. Bellamy, H. B. Greenberg, and P. H. Atkinson.** 1988. Two forms of VP7 are involved in assembly of SA11 rotavirus in endoplasmic reticulum. J. Virol. **62:**2929–2941.
23. **Kitamoto, N., R. F. Ramig, D. O. Matson, and M. K. Estes.** 1991. Comparative growth of different rotavirus strains in differentiated cells (MA104, HepG2, and CaCo-2). Virology **184:**729–737.
24. **Klumperman, J., A. Schweizer, H. Clausen, B. L. Tang, W. Hong, V. Oorschot, and H. P. Hauri.** 1998. The recycling pathway of protein ERGIC-53 and dy-

namics of the ER-Golgi intermediate compartment. J. Cell Sci. **111**(Pt. 22)**:** 3411–3425.
25. **Li, N., A. Mak, D. P. Richards, C. Naber, B. O. Keller, L. Li, and A. R. Shaw.** 2003. Monocyte lipid rafts contain proteins implicated in vesicular trafficking and phagosome formation. Proteomics **3:**536–548.
26. **Lopez, T., M. Camacho, M. Zayas, R. Najera, R. Sanchez, C. F. Arias, and S. Lopez.** 2005. Silencing the morphogenesis of rotavirus. J. Virol. **79:**184–192.
27. **Lopez, T., M. Rojas, C. Ayala-Breton, S. Lopez, and C. F. Arias.** 2005. Reduced expression of the rotavirus NSP5 gene has a pleiotropic effect on virus replication. J. Gen. Virol. **86:**1609–1617.
28. **McManus, M. T., and P. A. Sharp.** 2002. Gene silencing in mammals by small interfering RNAs. Nat. Rev. Genet. **3:**737–747.
29. **Michelangeli, F., F. Liprandi, M. E. Chemello, M. Ciarlet, and M. C. Ruiz.** 1995. Selective depletion of stored calcium by thapsigargin blocks rotavirus maturation but not the cytopathic effect. J. Virol. **69:**3838–3847.
30. **Midthun, K., H. B. Greenberg, Y. Hoshino, A. Z. Kapikian, R. G. Wyatt, and R. M. Chanock.** 1985. Reassortant rotaviruses as potential live rotavirus vaccine candidates. J. Virol. **53:**949–954.
31. **Mirazimi, A., and L. Svensson.** 1998. Carbohydrates facilitate correct disulfide bond formation and folding of rotavirus VP7. J. Virol. **72:**3887–3892.
32. **Mirazimi, A., C. H. von Bonsdorff, and L. Svensson.** 1996. Effect of brefeldin A on rotavirus assembly and oligosaccharide processing. Virology **217:**554–563.
33. **Nickel, W.** 2003. The mystery of nonclassical protein secretion. A current view on cargo proteins and potential export routes. Eur. J. Biochem. **270:** 2109–2119.
34. **Padilla-Noriega, L., R. Werner-Eckert, E. R. Mackow, M. Gorziglia, G. Larralde, K. Taniguchi, and H. B. Greenberg.** 1993. Serologic analysis of human rotavirus serotypes P1A and P2 by using monoclonal antibodies. J. Clin. Microbiol. **31:**622–628.
35. **Parashar, U. D., E. G. Hummelman, J. S. Bresee, M. A. Miller, and R. I. Glass.** 2003. Global illness and deaths caused by rotavirus disease in children. Emerg. Infect. Dis. **9:**565–572.
36. **Petrie, B. L., H. B. Greenberg, D. Y. Graham, and M. K. Estes.** 1984. Ultrastructural localization of rotavirus antigens using colloidal gold. Virus Res. **1:**133–152.
37. **Puertollano, R., and M. A. Alonso.** 1999. Targeting of MAL, a putative element of the apical sorting machinery, to glycolipid-enriched membranes requires a pre-Golgi sorting event. Biochem. Biophys. Res. Commun. **254:** 689–692.
38. **Roth, M. G., D. Gundersen, N. Patil, and E. Rodriguez-Boulan.** 1987. The large external domain is sufficient for the correct sorting of secreted or chimeric influenza virus hemagglutinins in polarized monkey kidney cells. J. Cell Biol. **104:**769–782.
39. **Sabara, M., L. A. Babiuk, J. Gilchrist, and V. Misra.** 1982. Effect of tunicamycin on rotavirus assembly and infectivity. J. Virol. **43:**1082–1090.
40. **Sapin, C., O. Colard, O. Delmas, C. Tessier, M. Breton, V. Enouf, S. Chwetzoff, J. Ouanich, J. Cohen, C. Wolf, and G. Trugnan.** 2002. Rafts promote assembly and atypical targeting of a nonenveloped virus, rotavirus, in Caco-2 cells. J. Virol. **76:**4591–4602.
41. **Schweizer, A., J. A. Fransen, T. Bachi, L. Ginsel, and H. P. Hauri.** 1988. Identification, by a monoclonal antibody, of a 53-kD protein associated with a tubulo-vesicular compartment at the cis-side of the Golgi apparatus. J. Cell Biol. **107:**1643–1653.
42. **Sevlever, D., S. Pickett, K. J. Mann, K. Sambamurti, M. E. Medof, and T. L. Rosenberry.** 1999. Glycosylphosphatidylinositol-anchor intermediates associate with Triton-insoluble membranes in subcellular compartments that include the endoplasmic reticulum. Biochem. J. **343**(Pt. 3)**:**627–635.
43. **Silvestri, L. S., Z. F. Taraporewala, and J. T. Patton.** 2004. Rotavirus replication: plus-sense templates for double-stranded RNA synthesis are made in viroplasms. J. Virol. **78:**7763–7774.
44. **Simons, K., and E. Ikonen.** 1997. Functional rafts in cell membranes. Nature **387:**569–572.
45. **Spangler, B. D.** 1992. Structure and function of cholera toxin and the related *Escherichia coli* heat-labile enterotoxin. Microbiol. Rev. **56:**622–647.
46. **Svensson, L., P. R. Dormitzer, C. H. von Bonsdorff, L. Maunula, and H. B. Greenberg.** 1994. Intracellular manipulation of disulfide bond formation in rotavirus proteins during assembly. J. Virol. **68:**5204–5215.
47. **Uduehi, A. N., S. H. Moss, J. Nuttall, and C. W. Pouton.** 1999. Cationic lipid-mediated transfection of differentiated Caco-2 cells: a filter culture model of gene delivery to a polarized epithelium. Pharm. Res. **16:**1805–1811.
48. **von Haller, P. D., S. Donohoe, D. R. Goodlett, R. Aebersold, and J. D. Watts.** 2001. Mass spectrometric characterization of proteins extracted from Jurkat T cell detergent-resistant membrane domains. Proteomics **1:**1010–1021.
49. **Xu, A., A. R. Bellamy, and J. A. Taylor.** 2000. Immobilization of the early secretory pathway by a virus glycoprotein that binds to microtubules. EMBO J. **19:**6465–6474.
50. **Zweibaum, A., N. Triadou, M. Kedinger, C. Augeron, S. Robine-Leon, M. Pinto, M. Rousset, and K. Haffen.** 1983. Sucrase-isomaltase: a marker of foetal and malignant epithelial cells of the human colon. Int. J. Cancer **32:**407–412.